AD-A282 051

ARMY RESEARCH LABORATORY

ARL

Site Competition Effect of Impurities and Grain Boundary Stability in Iron and Tungsten

Genrich L. Krasko

ARL-TR-452   June 1994

DTIC
ELECTE
JUL 21 1994
S G D

94-22578

94 7 19 054   DTIC QUALITY INSPECTED 1

REPORT DOCUMENTATION PAGE

Public reporting burden for this collection of information is estimated to average 1 hour per response, including the time for reviewing instructions, searching existing data sources, gathering and maintaining the data needed, and completing and reviewing the collection of information. Send comments regarding this burden estimate or any other aspect of this collection of information, including suggestions for reducing this burden, to Washington Headquarters Services, Directorate for Information Operations and Reports, 1215 Jefferson Davis Highway, Suite 1204, Arlington, VA 22202-4302, and to the Office of Management and Budget, Paperwork Reduction Project (0704-0188), Washington, DC 20503.

1. AGENCY USE ONLY (Leave blank)	2. REPORT DATE	3. REPORT TYPE AND DATES COVERED
	June 1994	

4. TITLE AND SUBTITLE
Site Competition Effect of Impurities and Grain Boundary Stability in Iron and Tungsten

5. FUNDING NUMBERS

6. AUTHOR(S)

Genrich L. Krasko

7. PERFORMING ORGANIZATION NAME(S) AND ADDRESS(ES)

U.S. Army Research Laboratory
Watertown, MA 02172-0001
ATTN: AMSRL-MA-CC

8. PERFORMING ORGANIZATION REPORT NUMBER

ARL-TR-452

9. SPONSORING/MONITORING AGENCY NAME(S) AND ADDRESS(ES)

U.S. Army Research Laboratory
2800 Powder Mill Road
Adelphi, MD 20783-1197

10. SPONSORING/MONITORING AGENCY REPORT NUMBER

11. SUPPLEMENTARY NOTES

12a. DISTRIBUTION/AVAILABILITY STATEMENT

Approved for public release; distribution unlimited.

12b. DISTRIBUTION CODE

13. ABSTRACT *(Maximum 200 words)*

Impurities, such as H, P, S, B, etc, have a very low solubility in iron and tungsten, and therefore prefer to segregate at the grain boundaries (GBs). In order to analyze the energetics of the impurities on the iron GB and the GB stability, the LMTO calculations were performed on a simple 8-atom supercell emulating a typical (capped trigonal prism) GB environment. The so-called "environment-sensitive embedding energies" were calculated for H, B, C, N, O, Al, Si, P, and S, as a function of the electron charge density due to the host atoms at the impurity site. It was shown that, at the electron charge density typical of a GB, both in Fe and W, boron and carbon have the lowest energy among the analyzed impurities, and thus would compete with them for the site on the GB, tending to push the other impurities off the GB.

14. SUBJECT TERMS
Site competition, Impurity grain boundary, Tungsten, Iron

15. NUMBER OF PAGES
11

16. PRICE CODE

17. SECURITY CLASSIFICATION OF REPORT	18. SECURITY CLASSIFICATION OF THIS PAGE	19. SECURITY CLASSIFICATION OF ABSTRACT	20. LIMITATION OF ABSTRACT
Unclassified	Unclassified	Unclassified	UL

13. ABSTRACT - continued

The effects of impurities on GB stability can be analyzed by simply comparing the GB energy differences, ΔE, between the GB with impurities and the CL GB. Our calculations show that both in Fe and W, the GB stability decreases from B towards O, and the energy difference becomes positive for Si, P and S (in Fe), and P and S (in W) --the strongest embrittlers. The latter means that GBs with the corresponding impurities make the GBs unstable at absolute zero.

Provided the technological difficulties can be overcome, microalloying with B could result in essential toughness improvements in current existing high-strength steels. 10-50 ppm of B can also make W less brittle.

Accesion For		
NTIS CRA&I	☑	
DTIC TAB	☐	
Unannounced	☐	
Justification		
By		
Distribution /		
Availability Codes		
Dist	Avail and / or Special	
A-1		

SITE COMPETITION EFFECT OF IMPURITIES AND GRAIN BOUNDARY STABILITY IN IRON AND TUNGSTEN

GENRICH L. KRASKO
U. S. Army Research Laboratory, Materials Directorate
Watertown, MA 02172-0001

Introduction

The reduced cohesion of grain boundaries (GBs) is often the controlling factor limiting ductility, and hence performance and reliability of high-strength metallic alloys (1). Intergranular embrittlement in metals is usually caused by impurities segregating towards the GBs (2-6). A ductile-brittle transition temperature (DBTT) as low as -196C (7) was observed in high purity W single crystals obtained by electron beam zone melting with special impurity gettering. Impurities present in bulk concentrations of 10^{-3}-10^{-4} atomic percent can result in a dramatic decrease of plasticity, drastically degrading mechanical properties of metallic alloys, and thus posing significant technological and application problems. This detrimental effect of minute impurity concentrations can be readily understood. A simple estimate shows that a ppm amount of impurity is sufficient for saturating all the grain boundaries in a typical grain-size polycrystal. Sensitivity of the DBTT to the grain size confirms the above physical concept: the larger the grain size, the smaller amount of impurity is needed to saturate the GB (3). Fine-grain polycrystals are known to be less brittle. It should be noted that BCC crystals, being not as close packed as FCC or HCP, are particularly prone to GB embrittlement by impurity segregation.

If impurities are the main cause of embrittlement, gettering the "the harmful" impurities, such as O, N, P, S, As, Sb, etc., from the GBs by their forming thermodynamically stable phases with other elements, is an obvious way of improving ductility. This process, however, requires careful control since the ductility upon gettering will be improved only so far as these second phase precipitates remain fine; any coagulation of precipitates, such as the so-called Ostwald ripening, would result in an adverse embrittling effect .

Fe-base alloys and W are among the most important ultra-high-strength materials. The purpose of this paper is to elucidate the energetics of impurities in Fe and W GBs, and analyze the effect of impurities on the intergranular cohesion at the electron-atom level. A deeper understanding of the cohesion-decohesion processes on the microscopic level will lay a foundation for a "smart design" of more ductile and tough alloys. In particular, our theoretical analysis of the electron structure and the energetics of Fe and W GBs, both clean (CL) and with impurities, enables one to make important predictions. Our calculations have shown that impurities, such as N, O, P, S, Si weaken the intergranular cohesion resulting in "loosening" of the GBs in Fe and W. The presence of B on the contrary, enhances the interatomic interaction across the GB. The so-called "site-competition effect" should play an important role affecting impurity distribution in GBs. Among the impurities analyzed, both in Fe and W, B in the GB has the lowest energy, and thus would tend to push other impurity atoms off the GB, thus improving resistance to brittle fracture.

Energetics of Impurities in Fe and W GBs and the Site Competition Effect

The progress in developing efficient methods of first-principles calculations and computational algorithms have made possible systematic studies of the role of impurities in

intergranular cohesion of transition metals at the atomic and the electron-ion level. Calculations on both cluster, two-dimensional and supercell models of GBs with impurities have provided an in-depth insight into mechanisms of GB decohesion (for references, see (8,9)).

Since the first-principles electronic calculations on low-symmetry systems (such as lattice defects or GBs) are still extremely complicated and costly, semi-empirical methods based on reliable first-principles foundations have also been developed. Among them, the most popular is the Embedded Atom Method (EAM) (10,11). This method has been successfully used in a wide variety of calculations.
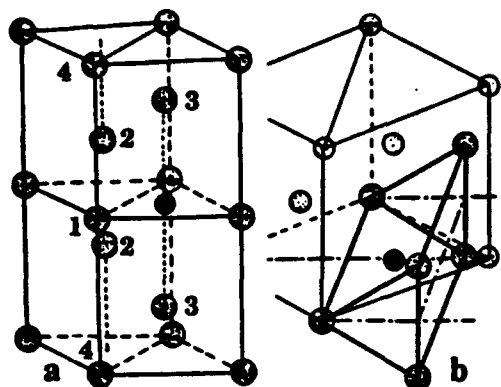

Fig. 1.The Me$_6$X hexagonal supercell emulating a typical trigonal prism environment of Fe or W atoms.in the (111)Σ3 GB: a) the supercell; b) the trigonal prism coordination; ⊗ Me, ● Impurity. Numbers designate atoms Me1 through Me4

In order to study the energetics of impurity atoms in Fe and W GBs, we have chosen first to calculate the quantity which may be called the "environment-sensitive embedding energy" (ESE) -- the energy of an impurity atom in an atomic environment typical for a GB. Knowledge of these energies for various impurities enables one to compare the relative stability of a particular impurity in the GB environment.

Having calculated the ESEs for a number of impurity atoms, one can use this information in a modified EAM approach for calculating the GB relaxation. The latter calculation enables one to draw important conclusions regarding the intergranular cohesion in Fe and W in the presence of a specific impurity in the GB.

The model chosen for the GB environment is an 8-atom hexagonal supercell (Me$_6$X, where Me is Fe or W, and X is an impurity atom). The supercell is shown in Fig.1, together with the capped trigonal prism coordination of the surrounding Me atoms.

A trigonal prism GB configuration is believed to be a typical GB environment in BCC metals and is predicted by the theory of hard sphere packing. Atomistic relaxation studies have shown that in Fe an impurity atom, such as P or B, is likely to occupy an interstitial position in the center of the trigonal prism formed by Fe atoms in the GB core (even if, like in the case of P and B, the impurity forms a substitutional solid solution with the host). The hexagonal supercell of Fig. 1 has a relatively high symmetry; it also emulates a (111) Σ3 GB environment (8). This model, however, does not allow segregation of tightly bound pairs of different impurity atoms.

We performed the spin-polarized scalar-relativistic Linear Muffin Tin Orbitals (LMTO) calculations (our method and approximations were the same as in (8)). First, a series of calculations (for six different volumes) were performed with an impurity absent from the supercell, i.e. an empty sphere of the same radius as that of the radius of the impurity's atomic sphere was substituted for the latter. Similar calculations were then performed for each of the impurities: H (Fe GB), B, C, N, O, Al, Si, P and S. The ESEs were defined as follows:

$$ESE = E(Me_6\bullet) - E(Me_6O) - E(\bullet) \tag{1}$$

where $E(Me_6\bullet)$ and $E(Me_6O)$ are respectively the energies of the supercell with and without the impurity (O stands for an empty sphere substituted for the impurity atom), and $E(\bullet)$ is the energy of the free impurity atom. In order to make the calculations more consistent, we have chosen to use, as $E(\bullet)$s, the values of $E(Me_6\bullet) - E(Me_6O)$ extrapolated to the zero charge density (n=0), which would correspond to the energies of impurities in the GB environment with the host crystal lattice infinitely expanded. The ESE energies, Eq.(1), as a function of n, the electron charge density due to the host atoms at the impurity site, are presented in Fig. 2.

Plots in Fig. 2 explain an experimentally observed phenomenon known as the "site competition effect ". As one can see, in the range of electron charge density typical of a Fe GB (0.015-0.025 a.u.), B and C have the lowest energy and thus would tend to displace the other impurities off the GB. Thus, there exists a "site competition hierarchy". In fact, in Fe, C is known to successfully compete with P

(12) and S (13,14), and N -- with P (15) and S (13). B should obviously be more efficient in pushing the harmful impurities off the GB. It was found recently (16,17) that B successfully competes with P. Since, in principle, ESEs are to be sensitive to the type and orientation of the GB, in some GBs B and C may compete in a reverse way. Also, it can be seen that H would successfully compete with all the impurities but B and C, N being a marginal case.

In W B has the lowest energy among the impurities analyzed, and the "gap" between B and C is significant. There is also a site-competition hierarchy. It was confirmed experimentally: N was found to successfully compete with C (18); while C competes with P (19).
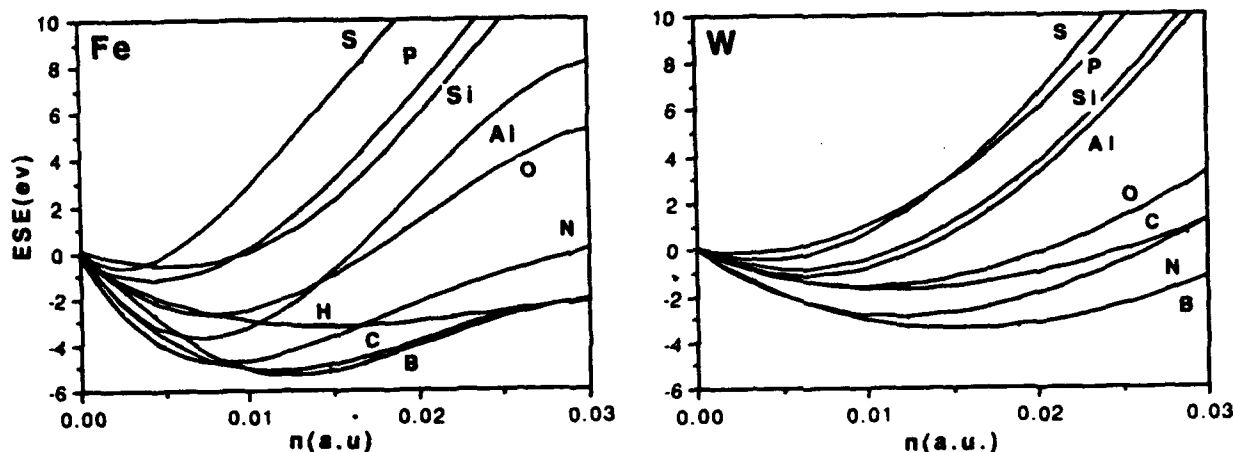

Fig. 2. The "environment sensitive embedding energies, ESE, vs n, the electron charge density (in atomic units)

The plots in Fig. 2 also reveal an important aspect of GB impurity behavior. All the plots have well pronounced minima. The positions of the minima correspond to the electron density at the impurity site due to the surrounding Me atoms which would occur if the GB were allowed to relax in such a way as to minimize the impurity's energy. The minima positions systematically (except for H in Fe) shift towards lower densities with the impurity losing its competitive power. A smaller charge density means a "looser" GB, less strong and more prone to decohesion. The minimization of the total GB energy (rather than only the energy of the impurity atom) gives the characteristic charge densities which are somewhat higher than those in the minima. However, from this point of view, N, O, S, P, Si and Al are the obvious candidates for being "decohesive", N is marginal, while B and C may be called "cohesion enhancers". In fact, B, C and N were experimentally found to improve the GB cohesion in both Fe (12-17) and W (18-22), while O, Si, P and S, being strong embrittlers both in Fe and W (3,6,23,24), are believed to weaken the GB cohesion .

As mentioned above, the GB environment we were dealing with was that of the (111) Σ3 tilt GB. The GB structure can be represented as a succession of (111) hexagonal planes:

....CBACBACBACBACBABCABCABCABCABC....

(the GB plane is marked by A). The CBABC atomic stacking of the core of the GB (CL or with an impurity) is just the one emulated by the 8-atom supercell shown in Fig.1. In order to find the GB structure corresponding to a minimum of energy, Eq.(2), the interplanar distances were varied, while the interatomic spacings and the structure within the (111) planes were left unchanged.

The total energy, E, was calculated using a modified EAM approach:

$$E = \Sigma_R\, E_{emb}(n(R)) + 1/2 \Sigma_{R,R'}\, V(R,R') + ESE(n(R_{imp}))$$ 　　　　(2)

where E_{emb} (n) and V(R,R') are the EAM embedding energy and the pair potential as found for the bulk BCC Me (we used the Finnis-Sinclair functions and parameters for Fe and W (11)). The third

term is the energy of the impurity atom. R and R' are the positions of the host atoms, R_{imp} is that of the impurity, and $n(R)$ and $n(R_{imp})$ are the electron charge densities at the site of a host atom and the impurity respectively. The electron charge density at a given site was taken to be a superposition of the free atom charge densities.

As follows from our calculations the volume difference between the CL GB and that with an impurity increases monotonically with the impurity atomic number. From the intuitive point of view, the increase in volume is expected to result in a weakening of interatomic bonding, though, in principle, an impurity may exert a stronger interaction in spite of the lattice expansion.
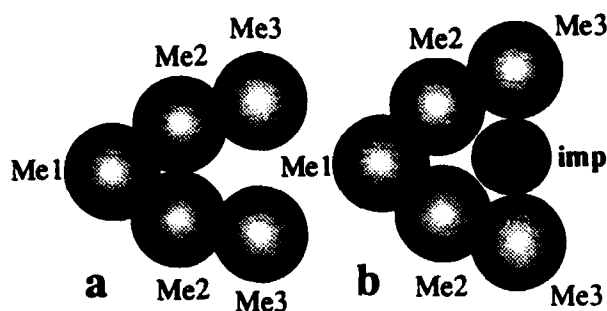

Fig. 3. Atom arrangements in GB cores:
a) CL GB; b) GB with an impurity atom

Fig. 3 schematically shows the atom arrangement in the GB core. The counterparts of the nearest neighbor distances in the bulk BCC lattice (0.2476nm in Fe and 0.2741nm in W) are the distances between nearest atoms in the [111] direction: Me1 and Me4 (Fe1-Fe4 and W1-W4 - see Fig.1). In the CL GBs these distances are larger than in the bulk, while the shortest distances are the ones between two Me2 atoms (Fe2-Fe2 and W2-W2) across the GBs. In the CL GBs there are significant voids (occupied by an empty sphere, O in our model); the distances between atoms Me3 across the void, and thus the GB plane, (Fe3-Fe3 and W3-W3) are quite large: 0.3108nm in Fe and 0.3614nm in W. Thus, in the CL GB the strongest interaction is Me2-Me2 across the GB, followed by Me1-Me4 and Me1-Me2. With an impurity atom in place of the empty sphere, the interatomic interaction fundamentally changes. Now the shortest distance is that between an impurity atom, ●, and Me3, the distance between two Me2 atoms across the GB being the second. The interaction between the impurity atom and atom Me3 becomes of utmost importance, since this is the interaction that is actually responsible for the intergranular cohesion: with the Me2-Me2 distances increasing, the main force that keeps the two halves of the crystal together is the one between the Me3 atoms via the impurity.

It was also found that, both in Fe (25) and W (26) GBs, the interplanar distances oscillate as a function of the distance from the GB, the deformation waves decaying by the 10th-12th plane away from the GB (plane 1 is the GB plane). An interesting feature of the CL GB relaxation is that the distance between the 2nd and 3rd planes is only a half of the (111) interplanar distance in bulk BCC Fe and W (0.0407nm vs 0.0825nm in Fe and 0.0550nm vs 0.0914nm in W). Though neither Fe nor W undergo transformation into the ω-phase, the "misbalance" in interatomic interactions arising due to the GB results in the tendency for plane 3 to nearly collapse into plane 2 (the ω-phase configuration).

Both in Fe and W, impurity atoms result in some "damping" of the relaxation deformation waves, i. e. decreasing the oscillation amplitudes. This damping is most pronounced for B and C. Although the distance between planes 1 and 2 (which is half the distance between two Me2 atoms across the GB) monotonically increases, the tendency of plane 3 to nearly collapse into plane 2 disappears: both in Fe and W, in the progression B through O the Me2-Me3 distance is almost equal to that in the bulk. Except for the Me2-Me3 distance, the amplitude of the deformation wave increases with Al, Si, P and S. Damping the deformation wave may be interpreted as "cohesion enhancement", while the corresponding increase of the deformation wave oscillations may be thought of as resulting in "decohesion".

These conclusions based on semi-empirical calculations also agree with our earlier first-principles analysis (8,9,26). It was shown that upon introducing an impurity atom in the GB the impurity's valence electrons hybridize with the Fe or W sp- and mostly d- electrons. As a result covalent bonds are created. Both in Fe and W, B happens to develop the strongest hybridization with the Me's electrons. The weakening of covalent bonds ●-Me3 (the most important for intergranular cohesion) with increase of the impurity's atomic number is most pronounced in Fe. H is known to be one of the strongest embrittlers in steels. The first-principles calculations (9) show that while the H-

Fe1 covalent bond (in the GB plane) is reasonably strong, the H-Fe3 bond, across the GB, is extremely weak. The hydrogen's only electron does not participate in metallic bonding. Contrary to a general belief, it is not transferred to Fe d-bands, but rather stays localized in the impurity band situated below the Fe valence bands.
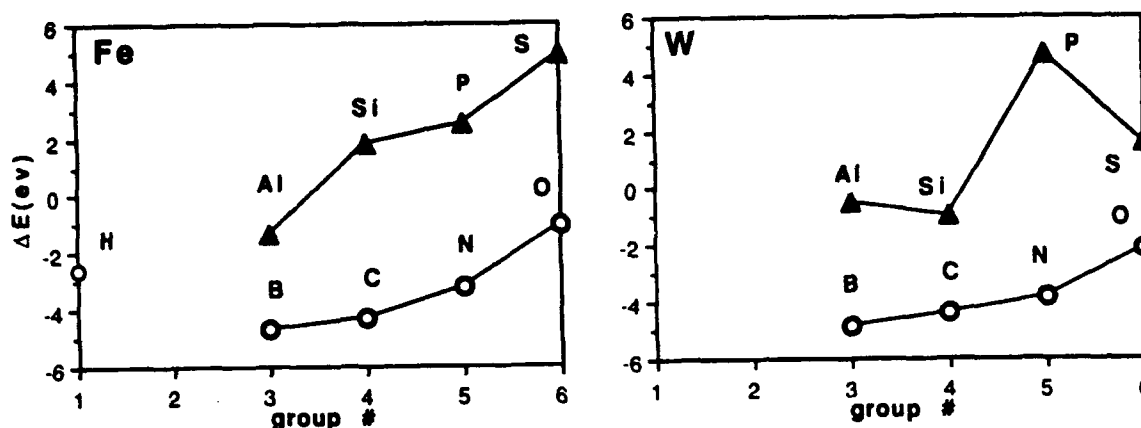

Fig. 4. $\Delta E = E_{GB}(\bullet) - E_{GB}(CL)$, the energy difference between the GB with impurity $\bullet$ and CL GB, vs the Periodic Chart group number.

The analysis of GB energetics reveals only one aspect of an impurity embrittling effect. From a thermodynamic point of view (27), the impurity's embrittling potency depends on the difference between the free energies of the impurity's segregation on the initial GB and on the two free surfaces emerging upon fracture. The higher the difference, the stronger the embrittling potency of the impurity. Thus, in order to have a complete thermodynamic picture of the embrittlement, one should be able to analyze the energetics of the same impurity on the free surface. As a much less rigorous but simpler criterion, in Ref.(5) the sublimation energy differences between the host and impurity atoms were calculated in an ideal solution model for over 60 elements. According to Ref. (5), among the elements analyzed, only B, C and Os may be cohesion enhancers in W. In Fe, over a dozen elements can play that role. In our more rigorous approach, the effects of impurities on GB stability can be analyzed by simply comparing the GB energy differences, ΔE, between the GB with impurities and the CL GB.

The corresponding values for the impurities discussed are plotted in Fig. 4. One can see that both in Fe and W, the GB stability decreases from B towards O, and the energy difference becomes positive for Si, P and S (in Fe), and P and S (in W) --the strongest embrittlers. The latter means that GBs with the corresponding impurities make the GBs unstable at absolute zero.

Conclusion

The site-competition effect is well known and experimentally observed in many systems. In this paper we made an attempt to understand this phenomenon on the microscopic, electron-atom level. From the theoretical point of view, the site-competition effect can be used in order to cleanse the GBs of the "harmful" impurities, such as P and S. Boron may be such a cleansing agent. Not only does it tend to displace other metalloid impurities from the GBs, it was also found to improve intergranular cohesion. This effect of boron has been observed in other systems also (26). An advantage of a "site competition" cleansing, as compared with traditional gettering, would be the absence of a second phase precipitate, which may be difficult to control. On the other hand, to "deliver" B to the GBs to be cleansed may be quite a difficult problem. In our analysis, we completely disregarded alternative chemical reactions of B both with the impurity and the matrix atoms that might result in formation of boron compounds, such as metal borides, boron oxides, etc. The thermodynamic analysis of the possibilities of such alternative reactions would be very helpful. We believe that an experimental investigation of the effect of B on ductility of Fe and W is of extreme importance. Recently (15,16), it was shown that B introduced in ppm quantities into an Fe-P alloy

significantly improves the alloy ductility. At the same time, the Auger analysis showed the decrease in the P concentration on the fracture surfaces -- a manifestation of the site competition effect. Provided the technological difficulties can be overcome, microalloying with B could result in essential toughness improvements in current existing high-strength steels. 10-50 ppm of B can also make W less brittle. Experimental research on microalloying W with B is currently in progress at Army Research Laboratory in Watertown, MA.

Acknowledgements

References

1. Embrittlement of Engineering Alloys (edited by C. L. Briant and S.K. Banerji), Acad. Press, New York, 1983; Interfacial Segregations, (edited by W.C. Johnson and J. M. Blakely), ASM, Metals Park, OH, 1979.

2. C. L. Meyers, Jr., G. Y. Onoda, A. V. Levy, and R. J. Kotfila, Trans. Metall. Soc. of AIME, **233**, 720 (1965).

3. J. Joshi and D. F. Stein, Metall. Trans, **1**, 2544 (1970).

4. D. A. Smith and G. D. W. Smith, in The Microstructure and Design of Alloys, Proc. of the 3rd Intl. Conf. on the Strength of Metals and Alloys, London, 1973, pp. 144-148.

5. M. P. Seah and E. D. Hondros, in Atomistics of Fracture (edited by R. M. Latanision and J. R. Pickens), Plenum, New York, 1983, pp. 855-888.

6. D. Y. Lee, E. V. Barrera, J. P. Stark and H. L. Marcus, Metall. Trans., **15A**, 1415 (1984).

7. Ye. M. Savitskiy and G. I. Burkhanov, Physical Metallurgy of Refractory Metals (Metallovedeniye Tugoplavkikh Metallov, in Russian), Nauka, 1967.

8. G. L. Krasko and G. B. Olson, Solid State Commun., **76**, 247 (1990).

9. G. L. Krasko and G. B. Olson, Solid State Commun., **79**, 113 (1991).

10. M. S. Daw and M. I. Baskes, Phys. Rev. **B29**, 6443 (1984); M. S. Daw, ibid, **39**, 7411 (1989).

11. M. W. Finnis and J. E. Sinclair, Phil. Mag., **A50**, 45, (1984,); ibid, **A53**, 161 (1986).

12. R. Möller, H. Hänsel, and H. J. Grabke, Scr. Metall., **18**, 527 (1984); H. J. Grabke, Scr. Metall., **20**, 1641 (1986); S. Suzuki, M. Obata, K. Abiko, and H. Kimura, Trans. Iron Steel Inst. Jpn., **25**, 62 (1985).

13. G. Tauber and H. J. Grabke, Ber. Bunsenges Phys. Chem., **82**, 198 (1978).

14. S. Suzuki, S. Tanii, K. Abiko, and H. Kimura, Metall Trans., **A18**, 1109 (1987); H. J. Grabke, Steel Research, **57**, 178 (1986); K. S. Shin and B. H. Tsao, Scr. Metall., **22**, 585 (1988)

15. H. Erhart and H. J. Grabke, Scr. Metall, **15**, 531 (1981).

16. C. M. Liu, T. Nagoya, K. Abiko, and H. Kimura, Metall. Trans. **23A**, 263 (1992).

17. K. Abiko and C. M. Liu, to be published.

18. L. S. Burmaka, A. S. Drachinskiy, Yu. I. Ivashchenko, V. G. Kostyuchenko, V. I. Trefilov and V. T. Cherepin, Physics of Metals and Metallography , **42**, 168 (1976).

19. H. Hoffman and S. Hoffman, Scripta Met. **18**, 77, (1984).

20. E. Smiti, P. Jouffrey, and A. Kobylanski, Scripta Met., **18**, 673 (1984).

21. C. L. White, J. R. Keiser, and D. N. Braski, Metall. Trans. **12A**, 1485 (1981).

22. K.B. Povarova, A. S. Drachinskii, Yu. O. Tolstobrov, A. V. Krainikov, V. N. Slyunyaev, V. A. Balashov, A. P. Popov, and K. I. Konovalov, Russian Metallurgy, Metally, No. 1, 129 (1987).

23. M. P. Seah, Acta Metall., **28**, 955 (1980).

24. T. H. Loi, J. P. Mornioli, M. Cantois, and M. Lahaye, J. Mat. Sci., **20**, 199 (1985).

25. G. L. Krasko,in Structure and Properties of Interfaces in Materials (edited by W. A. T. Clark, U. Dahmen and C. L. Briant), Mat. Res. Soc. Symp. Proc., **238**, Pittsburgh, PA, p.481 (1992).

26. G. L. Krasko, Proc. of the 1992 MRS Fall Meeting, Boston (to be published).

27. J. R. Rice and J.-Sh. Wang, Mat. Sci. and Engineering, **A107**, 23 (1989).

28. S. P. Chen, A. F. Voter, R. C. Albers, A. M. Boring, and P. J. Hay, J. Mater. Res., **5**, 955 (1990).

DISTRIBUTION LIST

No. of Copies	To

1   Office of the Under Secretary of Defense for Research and Engineering, The Pentagon,
     Washington, DC 20301

     Director, U.S. Army Research Laboratory, 2800 Powder Mill Road, Adelphi, MD 20783-1197
1   ATTN: AMSRL-OP-SD-TP, Technical Publishing Branch
1   AMSRL-OP-SD-TA, Records Management
1   AMSRL-OP-SD-TL, Technical Library

     Commander, Defense Technical Information Center, Cameron Station, Building 5,
     5010 Duke Street, Alexandria, VA 23304-6145
2   ATTN: DTIC-FDAC

1   MIA/CINDAS, Purdue University, 2595 Yeager Road, West Lafayette, IN 47905

     Commander, Army Research Office, P.O. Box 12211, Research Triangle Park,
     NC 27709-2211
1   ATTN: Information Processing Office

     Commander, U.S. Army Materiel Command, 5001 Eisenhower Avenue, Alexandria, VA 22333
1   ATTN: AMCSCI

     Commander, U.S. Army Materiel Systems Analysis Activity, Aberdeen Proving Ground,
     MD 21005
1   ATTN: AMXSY-MP, H. Cohen

     Commander, U.S. Army Missile Command, Redstone Arsenal, AL 35809
1   ATTN: AMSMI-RD-CS-R/Doc

     Commander, U.S. Army Armament, Munitions and Chemical Command, Dover, NJ 07801
1   ATTN: Technical Library

     Commander, U.S. Army Natick Research, Development and Engineering Center
     Natick, MA 01760-5010
1   ATTN: SATNC-MI, Technical Library

     Commasnder, U.S. Army Satellite Communications Agency, Fort Monmouth, NJ 07703
1   ATTN: Technical Document Center

     Commander, U.S. Army Tank-Automotive Command, Warren, MI 48397-5000
1   ATTN: AMSTA-ZSK
1   AMSTA-TSL, Technical Library

     President, Airborne, Electronics and Special Warfare Board, Fort Bragg, NC 28307
1   ATTN: Library

     Director, U.S. Army Research Laboratory, Weapons Technology, Aberdeen Proving Ground,
     MD 21005-5066
1   ATTN: AMSRL-WT

No. of Copies	To

Commander, Dugway Proving Ground, UT 84022
1   ATTN: Technical Library, Technical Information Division

Commander, U.S. Army Research Laboratory, 2800 Powder Mill Road, Adelphi, MD 20783
1   ATTN: AMSRL-SS

Director, Benet Weapons Laboratory, LCWSL, USA AMCCOM, Watervliet, NY 12189
1   ATTN: AMSMC-LCB-TL
1   AMSMC-LCB-R
1   AMSMC-LCB-RM
1   AMSMC-LCB-RP

Commander, U.S. Army Foreign Science and Technology Center, 220 7th Street, N.E., Charlottesville, VA 22901-5396
3   ATTN: AIFRTC, Applied Technologies Branch, Gerald Schlesinger

Commander, U.S. Army Aeromedical Research Unit, P.O. Box 577, Fort Rucker, AL 36360
1   ATTN: Technical Library

U.S. Army Aviation Training Library, Fort Rucker, AL 36360
1   ATTN: Building 5906-5907

Commander, U.S. Army Agency for Aviation Safety, Fort Rucker, AL 36362
1   ATTN: Technical Library

Commander, Clarke Engineer School Library, 3202 Nebraska Ave., N, Fort Leonard Wood, MO 65473-5000
1   ATTN: Library

Commander, U.S. Army Engineer Waterways Experiment Station, P.O. Box 631, Vicksburg, MS 39180
1   ATTN: Research Center Library

Commandant, U.S. Army Quartermaster School, Fort Lee, VA 23801
1   ATTN: Quartermaster School Library

Naval Research Laboratory, Washington, DC 20375
2   ATTN: Dr. G. R. Yoder - Code 6384

Chief of Naval Research, Arlington, VA 22217
1   ATTN: Code 471

Commander, U.S. Air Force Wright Research & Development Center, Wright-Patterson Air Force Base, OH 45433-6523
1   ATTN: WRDC/MLLP, M. Forney, Jr.
1   WRDC/MLBC, Mr. Stanley Schulman

U.S. Department of Commerce, National Institute of Standards and Technology, Gaithersburg, MD 20899
1   ATTN: Stephen M. Hsu, Chief, Ceramics Division, Institute for Materials Science and Engineering

No. of Copies	To
1	Committee on Marine Structures, Marine Board, National Research Council, 2101 Constitution Avenue, N.W., Washington, DC 20418
1	Materials Sciences Corporation, Suite 250, 500 Office Center Drive, Fort Washington, PA 19034
1	Charles Stark Draper Laboratory, 555 Technology Square, Cambridge, MA 02139
	Wyman-Gordon Company, Worcester, MA 01601
1	ATTN: Technical Library
	General Dynamics, Convair Aerospace Division, P.O. Box 748, Fort Worth, TX 76101
1	ATTN: Mfg. Engineering Technical Library
	Plastics Technical Evaluation Center, PLASTEC, ARDEC, Bldg. 355N, Picatinny Arsenal, NJ 07806-5000
1	ATTN: Harry Pebly
1	Department of the Army, Aerostructures Directorate, MS-266, U.S. Army Aviation R&T Activity - AVSCOM, Langley Research Center, Hampton, VA 23665-5225
1	NASA - Langley Research Center, Hampton, VA 23665-5225
	U.S. Army Vehicle Propulsion Directorate, NASA Lewis Research Center, 2100 Brookpark Road, Cleveland, OH 44135-3191
1	ATTN: AMSRL-VP
	Director, Defense Intelligence Agency, Washington, DC 20340-6053
1	ATTN: ODT-5A (Mr. Frank Jaeger)
	U.S. Army Communications and Electronics Command, Fort Monmouth, NJ 07703
1	ATTN: Technical Library
	U.S. Army Research Laboratory, Electronic Power Sources Directorate, Fort Monmouth, NJ 07703
1	ATTN: Technical Library
	Director, U.S. Army Research Laboratory, Watertown, MA 02172-0001
2	ATTN: AMSRL-OP-WT-IS, Technical Library
5	Author